Structures, energetics and magnetic properties of Au_nSFe_m and Au_nFe_m clusters for m = 1-5 and n = 1-5, 12 and 32

Hagos Woldeghebriel*
Department of Physics, CNCS, P.O.Box 231, Mekelle University, Mekelle, Ethiopia (*hagos93@mu.edu.et)

ABSTRACT

Simulations of nanoscale systems are important from the understanding point of view of the physics and chemistry involved in describing observed phenomenon. This paper presents the results of systematic theoretical investigation of the structural and magnetic properties of gold-iron complexes at small size scale. *Ab initio* calculations are performed for Au_nFe_m with and without the presence of a sulfur atom, i.e., the clusters Au_nSFe_m, where n, m = 1 - 5. The study also includes Au_6SFe and $Au_{12}Fe$ in order to investigate how the fully wrapped Fe atom responds to the Au atoms .The study mainly focuses on the geometrical and magnetic changes with a step by step removal of the sulfur atom as a function of the cluster size. It is found that average Au-Fe bond length is increased with increasing number of atoms in the cluster. An increase of Au-Fe bond length would have increased the magnetic moment of the Fe atom, but due to the hybridization of Au and Fe orbitals, the moment converges to about $3.00\mu_B$. This value is higher than the magnetic moment of Fe atom in bulk gold. An enhanced magnetic moment is found on Fe atom even if it is fully wrapped by the Au_{12} octahedral cluster. From this study it is found that, the cluster stability is increased on the addition of a single sulfur atom to the Au_nFe_m clusters. A special stability is observed in Au_4SFe, Au_6SFe, $Au_{12}SFe$ and Au_4SFe_2 clusters as the sulfur atom in these clusters is found to be doubly bonded. Generally, the systematic studies on the small sized clusters show an enhanced magnetic moment on the iron atoms bonded to the gold atoms as compared to the corresponding bare iron clusters. This indicates that, the magnetic moment of iron atoms can be enhanced by a complete coating with gold atoms for practical applications. This complete coating can prevent iron from oxidation and may also prevent coalescence of iron clusters and formation of thromboses. The coupling of iron atoms in this work remains ferromagnetic irrespective of the number of gold atoms in the cluster.

Keywords: Cluster, Magnetic moment, Coating, Nanoparticles.

1. INTRODUCTION

The presence of unfilled *d* shells of transition metal clusters has important consequences: *d* electrons give rise to more directional bonds and there are many low-lying excited states corresponding to the various possibilities to arrange the electrons in the empty *d* states. Properties, such as the stability of the cluster can often be discussed in terms of shells of atoms, relating the number of atoms needed to form a compact symmetric structure to an enhanced stability. If the *d* orbitals retain their atomic character and remain localized, the cluster will be magnetic. However, enhanced *s-d* and *d-d* hybridization will increase the tendency towards itinerant behaviour and decreases the local magnetic moments. Therefore, the magnetic moment

per atom will decrease (although nonmonotonically) with increasing cluster size, i.e., when atoms in the clusters have more nearest neighbors (Ganteför et al., 1996). Apart from molecular electronics (Häkkinen et al., 1999) and catalysis (Boccuzzi and Chiorino, 2000), gold-containing nanometer sized structures have exciting applications in the area of medical science (Sun et al., 2004) such as for cancer treatment. Conventional methods of treating malignant tumors such as surgery, radiation, and/or chemotherapy are either invasive or have adverse side effects. Nanostructural particles which have the same length scales as those of tumors provide some attractive possibilities where this noble goal may some day be achieved.

Sun et al. (2004) studied the effect of gold coating on the optical properties of a nanosilica cluster using time-dependent Density Functional Theory (DFT). They observed a reduction of the optical gap which makes it possible to absorb near infrared light (NIR). They termed this cluster as a "nanobullet for tumors" since it causes an irreversible thermal cellular destruction by conversion of the NIR light into heat and finally kills the cancer cells. Gold nanoparticles do not fluoresce but effectively scatter light, exhibiting a range of intense colors in the visible and NIR spectral region (Aizpurua et al., 2003). Gold nanoparticles are optically stable.

For a better efficiency of the cancer treatment, magnetically directed drug delivery combined with hyperthermia can greatly improve the performance of current procedures. An external magnetic field may be used to manipulate magnetic nanoparticles. The magnetic force acting on a point-like magnetic dipole ***m*** is defined by Vijay et al. (2008) as below.

$$\mathbf{F_m} = (\boldsymbol{m}\bullet\nabla)\mathbf{B} \qquad (1)$$

Where ***B*** is the magnetic induction. Ferromagnetic (FM) particles possess hysteretic properties when exposed to a time varying magnetic field, which gives rise to magnetically induced heating. The amount of heat generated per unit volume, P_{FM}, is given by the frequency, *f*, multiplied by the area of the hysteresis loop (Ortega and Pankhurst, 2013):

$$P_{FM} = \mu_0 f \oint H \bullet dM \qquad (2)$$

where ***H*** is the strength of the external magnetic field and ***M*** is the magnetization given by ***M*** = ***m***/*V* , magnetic moment per unit volume where ***m*** is the magnetic moment on a volume *V* of the nanoparticle and μ_0 is the permeability of free space. The strategy is to implant a nanoparticle near a cancer cell that can be heated through NIR light or an alternating magnetic field. The resulting heat can then destroy the tumor cells without damaging the healthy tissues. Since the

magnetic field can penetrate deep into the tissue, the use of magnetic fluid hyperthermia provides a versatile method to treat a variety of tumors such as anaplastic astrocytomas or glioblastomas. An ideal nanoparticle for this application should be a strong magnet which is biocompatible and resistant to corrosion as well as aggregation.

The conventional nanoparticles that are widely used in experiments and animal testing involve iron oxides. However, the magnetic strength of iron oxide is not as high as that of pure iron and there is significant interest in developing alternative high moment nanoparticles for specific biomedical applications. In fact, the ability to control size, shape, and composition of magnetic iron nanoparticles can provide flexibility for applications in cell labeling, magnetic resonance imaging (MRI), drug delivery and DNA separation (Mornet et al., 2004). Unfortunately, bare Fe particles cannot directly be used for the following reasons: (1) Free iron is toxic because of its propensity to induce the formation of dangerous free radicals. (2) They can easily aggregate to form larger particles, thus resulting in the formation of thromboses. (3) They can easily be oxidized, which in turn will weaken their magnetic property.

In another experimental study, gold-coated acicular and spherical shaped iron nanoparticles were characterized using transmission electron microscopy (TEM) and alternating gradient magnetometry. It has been found that the gold-coated nanoparticles were more resistant to oxidation and corrosion than the uncoated particles, and the gold shell was more uniformly distributed on the spherical particles than on the acicular ones (Chen et al., 2003).

In spite of these experimental studies, a fundamental understanding of how gold interacts with an iron core is still lacking. For example: (1) Does gold coating enhance or reduce the magnetic moment of iron and how does it change as the thickness of the coating is increased? (2) Do the iron atoms continue to couple ferromagnetically when the cluster is coated with gold? (3) Does the geometry of the iron core change when it is coated with gold? (4) How does the reactivity of Fe clusters toward oxygen change with Au coating? No experiments to my knowledge have measured the magnetic moment of a Fe core coated with gold.

On the theoretical front, very few studies have been carried out on noble metal coated metal nanoparticles. Tight binding based theoretical calculations (Guevara et al., 1999) were performed to understand the properties of Cu covered cobalt clusters. In a DFT based study, Wang et al. (2000) have investigated different magnetic properties of palladium coated and alloyed nickel clusters. Sun et al. (2006) reported the first theoretical investigation of the structural and

magnetic properties of gold-coated iron nanoparticles in various size ranges. They have shown that, coating of gold not only prevents the iron core from oxidation but also keeps the strong magnetic nature of iron alive. It is also observed that, the magnetic moment of the iron core is larger than its bulk value.

Magnetic particle hyperthermia is potentially the most significant and technically disruptive of the currently known biomedical applications of magnetic nanoparticles. Recent developments indicate that this highly specific and targetable method of localized remote heating of bodily tissue could revolutionize clinical practice in the treatment of cancer, either as an adjunct to radiotherapy and chemotherapy, or as a stand-alone intervention (Ortega and Pankhurst, 2013). Motivated by the practical application of gold-coated clusters, the author has studied computationally the interaction of small gold clusters with iron clusters.

2. COMPUTATIONAL DETAILS

First-principle calculations have been performed using pseudopotential method, as implemented in the QUANTUM ESPRESSO/ PWSCF package (http://www.pwscf.org), and DFT (Hohenberg and Kohn, 1964; Kohn and Sham, 1965). The electron-ion interaction was described by *ab-initio* using the projector augmented plane-wave (PAW) (Blöchl, 1994). PAW methods allow a considerable reduction in the number of plane-waves per atom for transition metals and first row elements and is more appropriate for simulations of systems containing transition metal elements. The PAW pseudopotential takes into account the relativistic effects as a contraction of the *s*-wave functions and an expansion of the *d*-wave functions. The total energy has been obtained by solving the standard Kohn-Sham (KS) equations using self-consistent method. The spin-polarized version of the generalized gradient approximation (GGA) is employed, as prescribed by Wang and Perdew (1991), for the exchange-correlation energy functional parameterized by Vosko et al. (1980). The valence wave function is expanded in the plane wave basis set with a kinetic energy cutoff of 280.00eV for the interaction of the Fe containing clusters. In the case of gold it is crucial to include 11 valence electrons ($5d^{10}6s^{1}$); for Fe 8 valence electrons ($3d^{7}4s^{1}$) are included and for sulfur 6 valence electrons ($3s^{2}3p^{4}$) are used in the calculations. The convergence criterion is considered to be 10^{-4}eV for the total electronic energy. A cubic supercell of size 20Å is taken for the small clusters and of size 24Å for the clusters with 12 Au atoms. Periodic boundary conditions are imposed on the box. The clusters are positioned at the center of the cell.

The Γ point is used to sample the Brillouin zone since a large supercell is employed. When the components of the forces on atoms are less than 0.005eV/Å, the structural optimization is taken to be converged. Structural optimizations are performed using a conjugate gradient method.

The calculation is carried out taking different starting geometries including 2D and 3D of Au_nFe_m and Au_nSFe_m clusters, with the restriction that, the S atom is bonded to one of the Au atoms through the S atom at the start of the simulation: The optimization of the cluster proceeds step by step to get the lowest energy structures of Au_nSFe_m and Au_nFe_m cluster. The goal is to study how the planar geometry of the gold cluster is affected by the dopants.

3. RESULTS AND DISCUSSION

The properties of neutral and cationic Au clusters and their interaction with H_2S molecule is described in Hagos and Anjali (2007a) and the interaction of a single sulfur atom with cationic Au clusters is discussed in Hagos and Anjali (2007b). In the present work, the interaction of neutral gold clusters with iron clusters in the presence and absence of S atom is investigated. The first part of this section deals with the *ab initio* calculation of possible geometries of Au_nFe clusters, (with n = 1 - 6, 12) with and without the presence of S atom. Then the number of Fe dopant atoms is increased in steps and the same calculation is repeated for each cluster. Geometrical structures, binding energies and magnetic properties are presented as a function of the number of gold atoms in the cluster for each Fe atom doped in the cluster. The bond length of Fe dimer in our calculation is 1.98Å and the magnetic moment is $2.82\mu_B$ which is in agreement with the results of Purdum et al. (1982), Castro and Salahub (1994), and Dièguez et al. (2001). To the best of my knowledge, there exists no report on the interaction of a single sulfur atom with a gold coated iron clusters. In order to understand the chemistry of the sulfur-gold and gold-iron interface, results of a gold coated or shielded iron nanoparticles in the presence and absence of a sulfur atom are presented.

3.1. Geometry and Magnetization

3.1.1.Au_nSFe and Au_nFe clusters

In figure 1 the calculated equilibrium geometries of the lowest energy structures of Au_nSFe and Au_nFe clusters for n = 1 - 6 along with $Au_{12}SFe$ and $Au_{12}Fe$ clusters are illustrated. These structures are found from possible 2D and 3D initial geometries considered in the calculation. In doing so, the initial geometries are prepared so that the sulfur atom is not connected to the iron

atom. During the process of simulation, though there is no restriction on movement of any atom, the sulfur atom remains connected to the gold atom where it was bonded at the start of the optimization. Exceptions are Au_4SFe and Au_6SFe clusters, shown respectively, in figures 1 (IV-a) and (VI-a). In these clusters the S atom is found to be doubly bonded to Au atoms. As shown in figure 1, the geometries of the clusters containing one Fe atom are all 2D structures with the exception of Au_6SFe cluster. In the structure of Au_6SFe cluster (VI-a), there are two planes, containing Au_4SFe and Au_4Fe, sharing two Au atoms (labeled by 2 and 5) and one Fe atom (labeled by 8) at the horizontal line, forming Au_2Fe cluster as a common side.

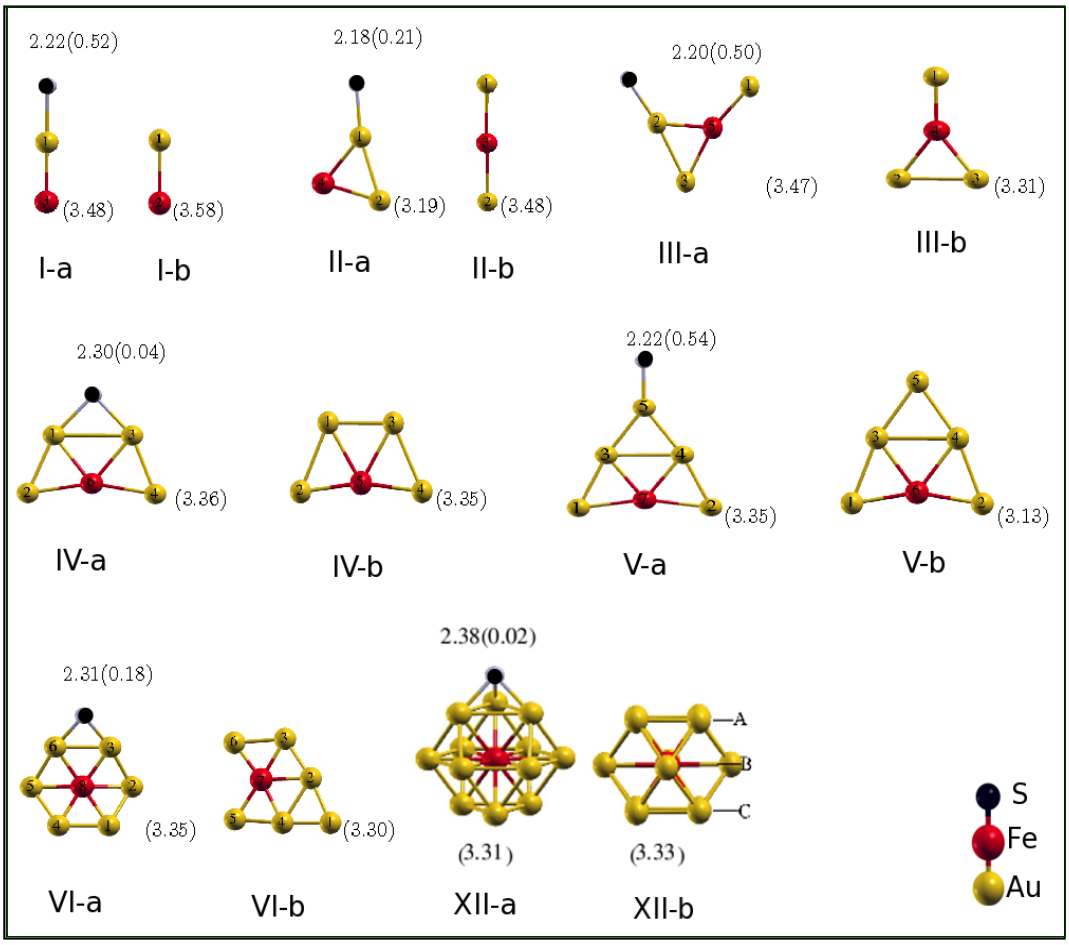

Figure 1. Optimized geometries for Au_nSFe, Au_nFe n = 1 - 6, $Au_{12}SFe$ and $Au_{12}Fe$ clusters. Specification of atoms is displayed at the bottom-right of this figure. Roman numbers represent number of Au atoms in the cluster. The number on top of a geometry represents Au-S bond length where as the number in brackets is the magnetic moment on S atom. The number in brackets at the bottom right of each cluster represents the magnetic moment on Fe atom.

The angle between the two planes is about 158^o, very large as compared to the angle between Au_5S^+ and Au_6 planes in the lowest energy structure of Au_8S^+ cluster as reported by Hagos and Anjali (2007b).

It is understood that the presence of an S atom in a relatively large gold cluster tends to bend the cluster for a better compactness leading to a 3D structure, for example Au_7S (Majumdar and Kulshreshtha, 2006) and Au_7S^+ (Hagos and Anjali, 2007b). However, in Au_6SFe cluster, the Fe atom prefers to be surrounded by the Au atoms. The tendency of the gold clusters to preferably have a 2D structure results in a slight bending so that greater bending angle is maintained between the planes. Generally, the presence of the Fe atom does not seem to affect the 2D nature of gold clusters as reported in Hagos and Anjali (2007a).

Recent studies have shown that, the structures of small gold clusters clearly differ from other coinage metal clusters: gold clusters prefer to be planar up to fairly large size (Häkkinen Landman, 2000). The preference for planar structure is related to the large mass of the gold atoms. Relativistic effects lower the energy and shrink the size of the 6*s* orbital, allowing a larger degree of 6*s*-5*d* hybridization and therefore stronger and more directional Au-Au bonds (Pyykkö, 1988). The overlap of the 5*d* orbitals is optimal for planar configurations. Magnetic moment of the Fe atom is shown in figure1 at the bottom right side of each cluster geometry. The Au-S bond length and the induced magnetic moment on the S atom are also shown in the same figure at the top of the respective geometries In all of the clusters presented here, the Fe atom does not prefer to be at the peripheral site of the structure. Au-S bond length is observed to be higher when the S atom is doubly and triply bonded with Au atoms than singly bonded.

In the single gold atom clusters, figure1 (I-a,b), the Fe atom forms a dimer with the gold atom. In the two Au atom clusters, figure 1 (II-a,b), the Fe atom tends to stay between the Au atoms, specially for the Au_2Fe cluster, the Au atoms lie on opposite sides of the Fe atom. The Fe atom in Au_3SFe and Au_3Fe clusters is also found to be sandwiched between the Au atoms, as shown in figure1 (III-a,b). For n = 4 and 5 the Fe atom is seen to go inside the gold cluster. The structure of Au_6Fe cluster is similar to the structure of neutral Au_7 cluster found in Hagos and Anjali (2007a). The even/odd oscillation of the Au-S bond length breaks at Au_4SFe cluster, where the S atom is found to be doubly bonded with two Au atoms. The average Au-Fe bond length is almost a constant for clusters with same *n*, except for *n* = 1 and 2. It is worth mentioning here that Sun et al. (2006) using the GAUSSIAN03 program found the Au-Fe bond length in AuFe dimer as

2.33Å and the magnetic moment of the Fe atom as 3.44μ_B. We found a magnetic moment of 3.58μ_B which is higher than their value, may be because of the higher bond length, 2.39Å, that is, found in this work. Another interesting observation in figure 1 is the induced magnetic moment on the S atom. There is a significant magnetic moment induced on the S atom in Au_nSFe clusters. The odd/even staggering of this moment is clearly seen with a very low value in the structure of Au_4SFe cluster. In general terms, the magnetic moment of the Fe atom in Au_nSFe clusters decreases with increasing *n* or with increasing coordination number. Greater bond length favors larger moment whereas increasing coordination of the Fe atom reduces its moment. The reduction of magnetic moment of the Fe atom in Au_nFe with increasing *n* is mainly due to the increasing coordination numbers although the average Au-Fe bond length also increases slowly. The Au atom in the AuSFe and AuFe clusters is found to be polarized ferromagnetically with respect to the Fe atom.

In the clusters with even number of gold atoms, all of the Au atoms are positively polarized. For n = 3, the two bonded Au atoms in Au_3Fe cluster are negatively polarized, whereas all Au atoms in Au_3SFe cluster are positively polarized. Similarly, in the clusters with n = 5, the gold atoms in Au_5SFe cluster are polarized positively, whereas in the other cluster, they are polarized negatively. The magnetic moment induced on the Au atom bonded to the sulfur atom in Au_nSFe clusters is found to be maximum. Due to the appreciable amount of induced magnetic moment on the sulfur atom in Au_nSFe clusters, it is found in this work that, generally, total magnetic moment of the clusters (μ_T) is more in Au_nSFe clusters as compared to Au_nFe clusters.

The geometry of the Au_{12}SFe cluster is shown in figure 1 (XII-a). The S atom is bonded to the three Au atoms with Au-S bond length of 2.38Å from each Au atom's site. The magnetic moment of the S and Fe atoms are 0.02μ_B and 3.31μ_B, respectively, and the total magnetic moment on the cluster is 3.69μ_B. The Fe atom of Au_{12}Fe cluster is fully wrapped in an octahedral shell of Au_{12} atoms as shown in figure 1(VII-b).

In summary, the maximum average Au-Fe bond length for Au_nFe clusters discussed above (*n*=1-6) is 2.58Å in Au_6Fe cluster, where the magnetic moment on the Fe atom is 3.30μ_B. For the Au_7Fe cluster the average Au-Fe bond length is 2.78 Å where the magnetic moment on Fe is found to be 3.33μ_B. Although the larger distance between Fe atom and Au atoms would cause the Fe moment to increase, the net reduction in the Fe moment with increasing number of Au

atoms is a result of hybridization of Fe 3*d* orbitals with 6*s* orbitals of the 12 Au atoms. The magnetic moment on the Fe atom is enhanced even more than the value, $3.00\mu_B$, reported by Sun et al. (2006) for Fe atom in an icosahedral shell. They found the Fe atom to be antiferromagnetically coupled to the Au atoms. It is interesting to note that the moment of a Fe impurity in bulk Au is found to be $3.05\mu_B$, while the moment of Fe in Fe-Au alloy is $2.95\mu_B$ (Khmelevskyi et al., 2004). Thus, one can conclude that, the magnetic moment of a Fe atom in Au has saturated to a value of about $3.00\mu_B$.

3.1.2. Au_nSFe_2 and Au_nFe_2(for n=1-4)

The geometries are shown in figure 2. Induced magnetic moment on the S atom, Au-S and Fe-Fe bond lengths along with the average magnetic moment of the Fe atoms are shown in the figure. The structure of $AuSFe_2$ is isosceles with Fe-Au-Fe angle of 49.9^o and is similar to the structure of Au_3Fe cluster shown in figure 1 (III-b) with Au-Fe-Au angle of 65.4^o. The Fe-Au-Fe angle in $AuFe_2$ cluster of figure 2 (I-b) is 46.5^o.

The geometries of Au_2SFe_2 and Au_2Fe_2 clusters are all 2D structures as shown in figure 2 (II). In such a planar structure the S atom in Au_nSFe_m clusters lie on the plane formed by the gold and iron atoms. It is worth mentioning here that, the Fe dimer bond length of Au_2Fe_2 cluster reported by Sun et al. (2006) is 0.26 Å more than that obtained in this work (2.03 Å). They have reported a higher magnetic moment, viz, 3.94 μ_B, on each of the Fe atoms. A similar geometry is found here with Fe dimer bond length equal to 2.26 Å but this geometry is found to be 0.17eV higher in energy than the structure shown in figure 2 (II-a).

The first 3D structure appears in the clusters containing three Au atoms as shown in figure 2 (III). In these clusters the Fe dimer remains surrounded by the Au atoms. The Fe dimer in Au_3SFe_2 cluster has one Au atom on one side and two Au atoms, one bonded to S atom, on the other side. The clusters containing four Au atoms are all 3D with the Fe dimer bounded by the Au atoms.

The structure of Au_4SFe_2 cluster shown in figure 2 (IV-a) is interesting. It is only in this cluster that we found the S atom bonded to an Fe atom. The average Fe-S bond length of this cluster is found to be 2.16 Å which is a bit smaller than the Au-Fe bond lengths.

Recent experiments suggest that gold-coated iron oxide nanoparticles can effectively bind with some sulfur containing amino acids such as cysteine and methionine (Kinoshita et al., 2005). These amino acids are responsible for some important biological functions. Sun et al. (2007) have studied theoretically the interaction of amino acids with gold coated iron oxide particles and

the effect of gold coating on the magnetic moments of the iron oxide core. They showed that, gold coating preserves the magnetism of the iron core while enhancing its stability. The gold coated iron oxide particle can selectively bind with sulfur containing amino acids. Molecules containing sulfur atoms are often used as surfactants, since they form particularly stable gold nanoclusters due to the strength of the gold sulfur bond. Stable iron sulfide clusters were found by Zhang et al. (1996) using photoelectron spectroscopy techniques.

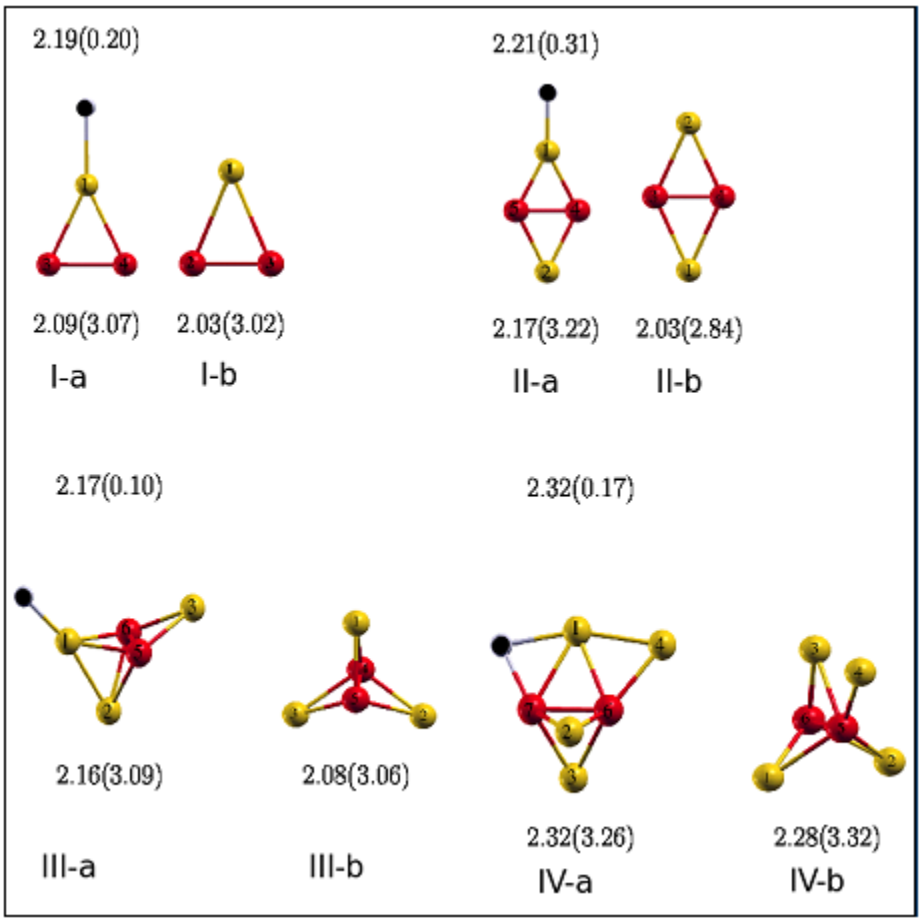

Figure 2. Optimized geometries for Au_nSFe_2 and Au_nFe_2 clusters, n = 1 - 4. Numbers at the bottom of each cluster denote the Fe-Fe bond length with the numbers in bracket giving the average magnetic moment of the Fe dimer. The numbers at the top of a cluster gives the Au-S bond length and the numbers in bracket are the moment on the S atom.

Au-S bond length of the Au_nSFe_2 clusters show odd/even alternation with increasing, *n*, the number of Au atoms. Au_nSFe_2 clusters with an even *n* have greater Au-S bond length as compared to their correspondingly nearest clusters of ($n \pm 1$) atoms. An increase of the average

Au-Fe bond length in Au_nSFe_2 clusters and a decrease in Au_nFe_2 clusters with increasing *n* is seen in this work.

Induced magnetic moment on S atom is found to be appreciable in Au_nSFe_2 clusters and it shows an odd/even alternation parallel to the Au-S bond length pattern. In all of the clusters, Au atoms are found to be positively polarized. The Fe atom at a shorter distance from the Au atom has less magnetic moment in Au_4SFe_2 cluster, the coordination of the two Fe atoms is the same but since the Fe-S bond length is shorter than the Au-Fe bond length, the Fe atom bonded to the S atom is found to possess smaller magnetic moment.

An odd/even alternation of the average magnetic moment of the Fe dimer is seen in the Au_nSFe_2 clusters as shown at the bottom of each structure shown in figure 2. The coordination number of the two Fe atoms in Au_4Fe_2 cluster is not the same. Since the magnetic moment is less for a larger coordination number, we should expect different values of magnetic moment for these two Fe atoms, lesser in the five coordinated atom. But the other factor, namely, a greater bond length enhances the magnetic moment of the Fe atom with larger coordination number and as a result the magnetic moments of the two Fe atoms are the same.

Another observation of figure 2 gives a very interesting relationship between the average magnetic moment of the Fe dimer and the Fe dimer bond length with increasing number of Au atoms in each of the two species. The greater bond length favoring enhanced magnetic moment is visibly seen except for Au_2Fe_2 cluster. A clear picture of the trend is shown especially in Au_nSFe_2 clusters. In general, the Fe-Fe bond length increases with increasing number of Au atoms in the cluster and the magnetic moment of the Fe dimer is enhanced relative to the magnetic moment of the bare Fe dimer.

3.1.3. Au_nSFe_3 and Au_nFe_3 (for n = 1 - 3)

Geometries of the clusters containing three Fe atoms are shown in figure 3. In the structure of Au_2SFe_3 cluster, that is, figure 3 (II-a) is a growth over the $AuSFe_3$ cluster, but the planar structure of Au_3SFe_3 cluster, that is, figure 3 (III-a) is not grown from Au_2SFe_3 cluster. The removal of the S atom from the 3D structure of $AuSFe_3$ and Au_2SFe_3 clusters changes the structures of $AuFe_3$ and Au_2Fe_3 clusters back to 2D structures.

As shown in figure 3, the Au-S bond length, given on top (out of bracket) of the clusters containing S varies slowly with increasing the number of Au atoms. Inspite of the small increase in Au-S bond length, the induced magnetic moment on the S atom increases with

increasing *n* in Au_nSFe_3 clusters. If one observes the average Fe-Fe bond length shown at the bottom of each cluster geometry in figure 3, there is little change with *n* for each species. However, the magnetic moment of the Fe atoms, given at the bottom in brackets of each cluster geometry is found to be sensitive to these changes. Accordingly, the average magnetic moment of the Fe atoms in Au_nSFe_3 clusters increases as the average Fe-Fe bond length increases with increasing *n*. In figure 3 (II-a,b), one can observe that, there is hardly any effect on the average magnetic moment of the Fe trimer whether the cluster contains an S atom or not. All Au atoms of Au_nSFe_3 and Au_nFe_3 clusters are ferromagnetically polarized with respect to the orientation of the magnetic moment on Fe atoms. The Au atoms are polarized less as compared to the structures containing two Fe atoms discussed above.

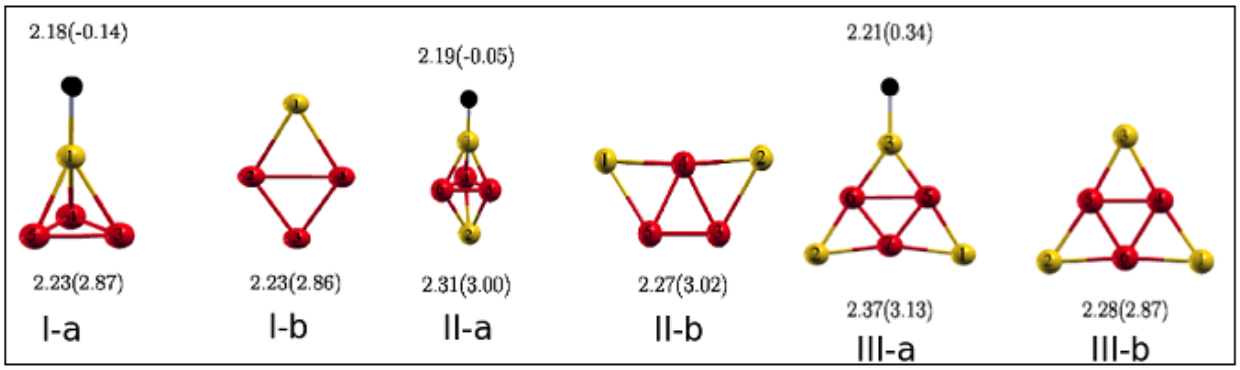

Figure 3. Optimized geometries for Au_nSFe_3 and Au_nFe_3 clusters, n = 1 - 3. Numbers at the bottom of each cluster denote average Fe-Fe bond length with the number in brackets giving the average magnetic moment of the Fe trimer. The numbers at the top of a cluster are the Au-S bond length and the moment on the S atom (in bracket).

3.1.4. Au_nSFe_4, Au_nFe_4, $AuSFe_5$ and $AuFe_5$ (for n = 1 - 2)

These clusters appear to be all 3D structures as shown in figure 4. Symmetrical positions of the two Au atoms are seen in Au_2Fe_4 cluster. The structures of the clusters containing two Au/four Fe atoms and the clusters with one Au/five Fe atoms are similar in their respective species as shown in the figure 4. On paying due attention to figures 4 (I-a,b) and 3 (I-a,b), we can say that the structures of $AuSFe_4$ and $AuFe_4$ clusters are, respectively, derivatives of the structures of $AuSFe_3$ and $AuFe_3$ clusters. It is also shown that $AuSFe_3$ and $AuFe_3$ clusters are building blocks for the growth of the clusters containing three Fe atoms shown in figures 3, but not for Au_3SFe_3 cluster. Therefore, we can say that, these clusters, namely $AuSFe_3$ and $AuFe_3$ generally serve as building blocks for the growth, respectively of Au_nSFe_m and Au_nFe_m, for $m \geq 3$ clusters.

As shown in figure 4, the average Fe-Fe bond length increases with the total number of atoms in the cluster for each species. The same observation is seen with the increase of Fe atoms as well. Most important observation in this work is that, the Au atoms prefer to be on the peripheral side than the Fe atoms in the cluster. In other words, the Au atoms are trying to surround the Fe clusters leaving the structure of the Fe atoms undisturbed (Author also optimized bare Fe clusters up to m = 6, not included in this work). The geometries are similar to the geometries of the Fe_m part of the clusters presented here with slight structural modifications around the Au atom(s) in the latter. The unperturbed structure of Fe atoms after Au coating is important for practical applications.

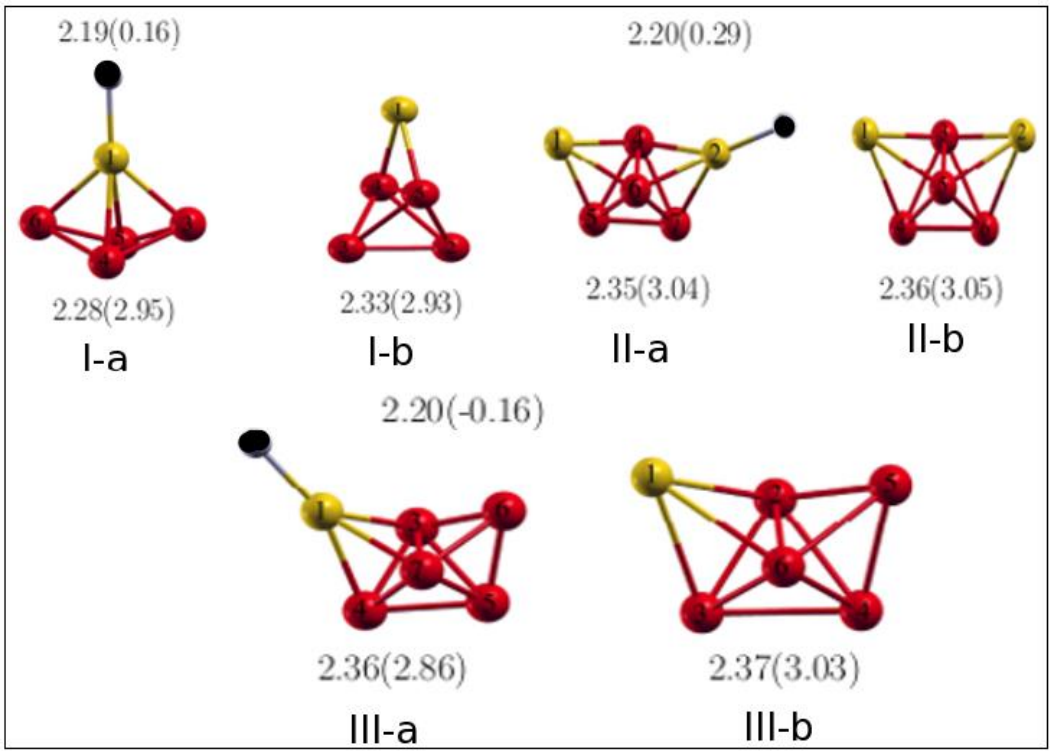

Figure 4. Optimized geometries for Au_nSFe_4 and Au_nFe_4 clusters, with n = 1 - 2, and for $AuSFe_5$ and $AuFe_5$ clusters. Numbers at the bottom of each cluster denote average Fe-Fe bond length, with the number in brackets giving the average magnetic moment of the Fe cluster. The numbers at the top of a cluster are the Au-S bond lengths and the moments on the S atom (in bracket).

Induced magnetic moment on the S atom in the clusters shown in figure 4 are values, being negative in $AuSFe_5$ cluster. The Au atoms are all polarized ferromagnetically with respect to the magnetic moment of the Fe atoms. There is a clear relationship between the average Fe-Fe bond length and the average magnetic moment on the Fe atoms as shown in figure 4, that is, the

greater the average Fe-Fe bond length, the greater is the average magnetic moment on the Fe atoms. The Au-Fe bond length in all the clusters is shorter than the corresponding Au-Au bond lengths, due to the smaller radius of the Fe atom. Due to the larger covalent radius of Au(1.44Å) than Fe(1.27Å) (Kittel, 1996), the Fe atoms prefer to be bounded by the Au atoms.

Table 1. Average Fe-Fe bond length in (a) Au_nSFe_m and (b) of Au_nFe_m clusters. The arrows indicate how the Fe-Fe varies with varying the number of Au (n) and Fe (m) atoms in the clusters.

m									
5	2.36				2.37				
4	2.28	2.35			2.33	2.36			
3	2.23	2.31	2.37		2.23	2.27	2.27		
2	2.09	2.17	2.16	2.32	2.03	2.03	2.08	2.28	
	1	2	3	4	1	2	3	4	n

(a) (b)

Table 2. Average Au-Fe bond length in (a) Au_nSFe_m and (b) Au_nFe_m clusters respectively. The arrows indicate how the Au-Fe varies with varying the number of Au (n) and Fe (m) atoms in the clusters.

m									
5		2.56							
4		2.65	2.59						
3		2.56	2.60	2.50					
2		2.48	2.51	2.55	2.58				
1		2.35	2.44	2.45	2.52	2.51	2.63	2.80	
		1	2	3	4	5	6	12	n

(a)

m									
5		2.60							
4		2.54	2.60						
3		2.56	2.53	2.52					
2		2.57	2.56	2.56	2.52				
1		2.39	2.37	2.46	2.52	2.54	2.58	2.76	
		1	2	3	4	5	6	12	n

(b)

Results can be summarized by displaying the average bond length between the iron atoms in the clusters and the average magnetic moment on the Fe atoms as a function of the number of Au and Fe atoms in the cluster as shown in tables (1) to (3) in a matrix form. The average Fe-Fe

bond length as shown in table 1 (a) for Au_nSFe_m clusters and table 1 (b) for Au_nFe_m clusters is found to increase with increasing number of Au atoms (horizontal) and number of Fe atoms (vertical), but the change in Au_nFe_m clusters is fast or is dominated by the number of Fe atoms as shown by the diagonal arrow in (b). Though, the Fe-Fe bond length increases on the average with increasing number of gold atoms in the cluster, the strong reduction of Fe-Fe bond length compared to the bulk nearest-neighbor distance of 2.48 Å is evident.

The average Au-Fe bond length, table 2(a) of Au_nSFe_m clusters, decreases with decreasing number of Fe atoms (except for m=4) and increases with increasing number of Au atoms (except for m=5) and no conclusion can be drawn as to whether *n* or *m* dominates the change. Average Au-Fe bond length of Au_nFe_m clusters increases with the increase of Au and Fe atoms in the clusters, but similar to Au_nSFe_m clusters no conclusion can be drawn as to whether *n* or m dominates the change.

Table 3. Average magnetic moment of Fe atom in (a) Au_nSFe_m and (b) Au_nFe_m clusters. The arrows indicate how the magnetic moment varies with varying the number of Au (n) and Fe (m) atoms in the clusters.

m							
5	2.86						
4	2.96	3.04					
3	2.87	3.00	3.13				
2	3.07	3.22	3.09	3.26			
1	3.48	3.19	3.47	3.36	3.35	3.35	3.31
	1	2	3	4	5	6	12 n

(a)

m							
5	3.03						
4	2.93	3.05					
3	2.86	3.02	2.87				
2	3.02	2.84	3.06	3.33			
1	3.58	3.48	3.31	3.35	3.13	3.33	3.30
	1	2	3	4	5	6	12 n

(b)

Table 3 (a) and (b) displays average magnetic moment of the Fe atom in Au_nSFe_m and Au_nFe_m clusters, respectively. In both species, the magnetic moment generally decreases as the number of Au and Fe atoms increase. In particular the situation in tables 2(b) and 3(b) are opposite, increase in Au-Fe bond length results in decreasing magnetic moment in Fe atom. In this study,

an enhancement of the magnetic moment of the Fe clusters is observed, on coating with the Au atoms, by about 1.3% to 17.0% (discussion of bare Fe clusters is not included in this work).

In general, the average magnetic moment in Fe atom seems to decrease slowly and converges to a value greater than $3.00\mu_B$, which is the magnetic moment of a Fe impurity in bulk Au (Khmelevskyi et al., 2004). Thus, one could conclude that, the magnetic moment of Fe in Au has saturated to a value greater than the value in bulk iron. This study shows that, the coupling between the Fe atoms remains ferromagnetic irrespective of the number of gold atoms and the presence of the S atom in the clusters. However, whenever the Au atoms are antiferromagnetically coupled with the Fe atoms or not, the magnetic moment of the Fe atom is observed to be smaller in comparison to the situation when they are ferromagnetically coupled. The trend of the average magnetic moment of the Fe atoms is similar to that of the total magnetic moment of the clusters as discussed earlier.

This study includes the simulation of $Au_{32}Fe_6$ spherically symmetrical cluster where the Fe atoms are found to be completely covered by the Au atoms as shown in figure 5. The size of the cluster is on the average 8.4Å in diameter, where as the average Fe-Fe and Au-Fe bond lengths are respectively 2.39Å and 2.78Å. The average magnetic moment on the Fe atoms is found to be $3.20\mu_B$ which is greater than the bulk iron. This bigger cluster is still found to provide an appreciable amount of magnetic moment on the Fe atoms which justifies the convergence of the magnetic moment to about $3.00\mu_B$.

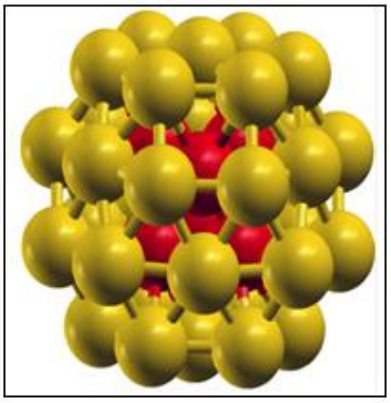

Figure 5. Optimized geometry of $Au_{32}Fe_6$ cluster.

3.2. Binding Energy

In this work, the stability of the clusters shown in figures 1 to 4 are discussed based on the calculated binding energy (BE) using the following two equations.

$$BE = \frac{nE(Au) + E(S) + mE(Fe) - E(Au_nSFe_m)}{n+m+1} \quad (3)$$

where *n* and *m* stand for the number of Au atoms and the number of Fe atoms in the cluster respectively. Equation (3) evaluates the binding energy of all clusters of the form Au_nSFe_m, and equation (4) given below,

$$BE = \frac{nE(Au) + mE(Fe) - E(Au_nFe_m)}{n+m} \quad (4)$$

is used to evaluate the binding energy of all clusters of the form Au_nFe_m. The binding energy curves are shown in figure 6.

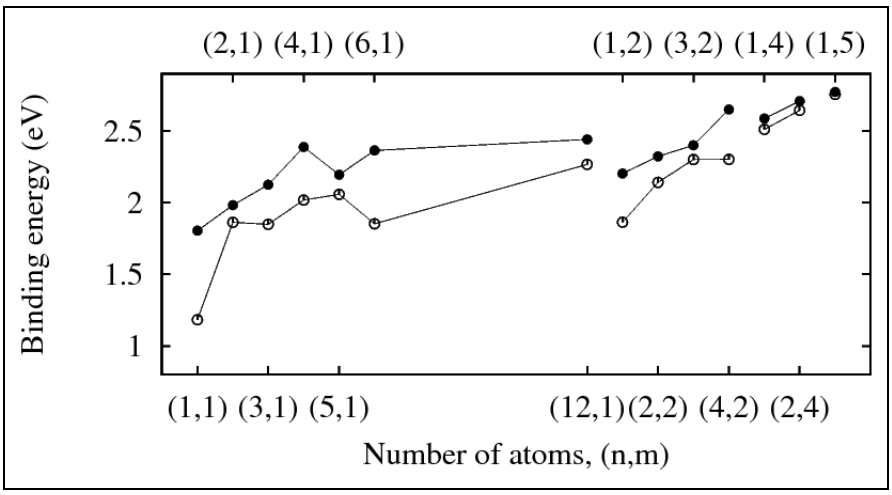

Figure 6. Binding energy as a function of n and m, the number of Au and Fe atoms in the clusters. Open circles and solid circles are the binding energies of Au_nFe_m and Au_nSFe_m clusters, respectively. Figures are separated in groups along the horizontal axis according to the number of Fe atoms present in each group.

For fixed *m* of Fe atoms in each species, the binding energy increases with increasing the number of Au atoms as shown in figure 6. However, the increase in the binding energy is slow for large number of atoms. The binding energy of Au_nSFe_m clusters show greater binding energy as compared to the Au_nFe_m species for the same *n* and *m*. But Au_4SFe, Au_6SFe, $Au_{12}SFe$ and Au_4SFe_2 clusters have special stability. From the geometry of the clusters, it is seen that, the S atom is bonded to two Au atoms in the clusters Au_4SFe, Au_6SFe and $Au_{12}SFe$ as shown in figure 1 Therefore, the higher binding energy of these clusters is attributed to the strong bond between the S atom and gold clusters. Similarly, the S atom is seen bonded to a Fe atom in Au_4SFe_2

cluster shown in figure 2(IV-a). This is in agreement with the experimental result of Zhang et al. (1996). They observed stable iron sulfide clusters using photoelectron spectroscopy techniques. In Au_nFe_m clusters, the Au_2Fe cluster shows enhanced binding energy which is also reflected in the Au-Fe bond length. In this family of clusters, the average Au-Fe bond length is small in Au_2Fe cluster.

Table 4. Binding energy matrix of (a) Au_nSFe_m and (b) Au_nFe_m as a function of (n,m). The arrows indicate how the magnetic moment varies with varying the number of Au (n) and Fe (m) atoms in the clusters.

m								
5	2.774							
4	2.588	2.709						
3	2.428	2.525	2.568					
2	2.204	2.323	2.401	2.651				
1	1.805	1.983	2.125	2.389	2.195	2.365	2.442	
	1	2	3	4	5	6	12	n

(a)

m								
5	2.756							
4	2.512	2.645						
3	2.223	2.417	2.540					
2	1.864	2.142	2.301	2.302				
1	1.182	1.863	1.849	2.019	2.058	2.005	2.267	
	1	2	3	4	5	6	12	n

(b)

From tables 4 (a) and (b), it can be shown that the binding energy increases with the increase of number of Au(except for n=5 in 4(a) and n=3 and n= 6 in 4(b)) and Fe atoms in the respective clusters but the change is dominated by the increase in number of Fe atoms in the clusters shown by the diagonal arrow, similar to the average Fe-Fe bond length displayed in table 1.

4. CONCLUSION

This paper presents *ab initio* calculations to study the equilibrium geometries, electronic structure and magnetic properties of the gold-iron hetro-clusters. The specific clusters used are of the form Au_nFe_m and Au_nSFe_m clusters. Generally, it is found that, the use of one Fe atom in the small clusters ($n \leq 6$) results in a 2D structure for the Au_nFe part of the clusters at the small size. The 2D nature of Au_n clusters is not affected by the addition of one Fe atom.

In the structures of Au_4SFe and Au_6SFe clusters, the S atom is found to be doubly bonded where as the cluster $Au_{12}SFe$ is triply bonded to Au atoms. These clusters are found to be more stable

as the S atom increases the stability of Au clusters. In the other small clusters, the S atom is bonded to a single Au atom only. The Au-S bond length is greater in the clusters where the S atom is doubly bonded with the Au atoms as compared to the other Au_nSFe_m clusters. The average Au-Fe bond length is seen to increase with the increasing number of atoms in the clusters. The increase of Au-Fe bond length is expected to increase the magnetic moment of a Fe atom, but due to the hybridization of Au and Fe orbitals, the moment converges to about $3.00\mu_B$. However, an enhanced magnetic moment is found on the Fe atom when it is fully wrapped by the Au_{12} octahedral cluster and the spherically symmetrical Au_{32} cluster. For values of $m \geq 2$, 3D structures start at $(n,m) = (3,2)$ clusters.

In this work, the spectrum of the graphs of Fe-Fe bond length plotted against the combination of (n,m), the number of Au and Fe atoms respectively in the cluster, shows an increase in the average Fe-Fe bond length. From this study it is found that, the cluster stability increases on addition of a single S atom to the Au_nFe_m clusters. A special stability is found in Au_4SFe_2 cluster since its S atom is bonded to Au and Fe atoms. The introduction of the S atom makes the Au-S bonding more favorable, as the 3*p* energy level in S is significantly closer to the 6*s* orbital energy in Au. The human body also contains sulfur (mainly in the proteins distributed in all cells and tissues) and can easily bind to gold which is biocompatible for functionalization. Moreover, during the interaction with Au atoms, it is found no visible structural changes in the geometry of the iron clusters which are reported by Dièguez et al. (2001) except for some re-orientations around the Au-Fe interface. Based on the electronegativity of Au and Fe, the bonding between Au and Fe is said to be ionic.

To summarize the results, small clusters containing Au and Fe atoms are studied which can be used in biomedical applications. An enhanced magnetic moment is found on the Fe site when bonded to the Au atoms as compared to bare Fe atoms. This leads to a conclusion that, the magnetic moment of Fe atoms can still be enhanced by completely coating with Au atoms for practical applications, as is seen in $Au_{32}Fe_6$ cluster (Fig 5). This complete coating can prevent iron from oxidation and may also prevent their coalescence and formation of thromboses. Magnetic nanoparticles are now routinely used as contrast agents for the mononuclear phagocyte system (MPS organs) (liver, spleen and bone marrow) and very soon for lymph nodes. It is obvious that, future developments will be in the direction of active targeting through molecular imaging and cell tracking. Therefore, in the case of cancer diagnosis, the next challenge for the

future is the generation of functionalized surfaces of these particles. Finally, this work can be closed by hoping that, these nanoparticles may bring a fundamental solution in the very near future for the cancer patients in the world.

5. ACKNOWLEDGEMENTS

The author would like to thank the Department of Physics at the College of Natural and Computational Sciences, Mekelle University, Ethiopia, for providing computational facilities to conduct the research work.

6. REFERENCE

Aizpurua, J., Hanarp, P., Sutherland, D.S., Käll, M., Bryant, G.W & Garciía de Abajo, F.J. 2003. Optical properties of gold nanorings. *Phys. Rev. Lett.,* **90**:057401.

Blöchl, P.E. 1994. Projector Augmented-Wave Method. *Phys. Rev. B,* **50:**17953.

Boccuzzi, F & Chiorino, A. 2000. FTIR Study of CO Oxidation on Au/TiO_2 at 90 K and Room Temperature: An Insight into the Nature of the Reaction Centers. *J. Physical Chemistry B,* **104(23):** 5414-1516.

M. Castro, M & Salahub, D.R. 1994. DENSITY-FUNCTIONAL CALCULATIONS FOR SMALL IRON CLUSTERS - FEN, FEN- FOR N-LESS-THAN-OR-EQUAL-TO-5(, AND FEN). *Physical review. B, Condensed matter*, **49(17)**: 11842-11852.

Chen, M., S., Yamamuro, D. Farrell, & Majetich, S.A. 2003. Gold-Coated Iron Nanoparticles for Biomedical Applications. *Journal of Applied Physics,* **93(10)**: 7551-1753.

Cho, S. J, Idrobo, J.C., Olamit, J., Liu, K., Browning, N.D & Kauzlarich, S.M. 2005. Growth Mechanisms and Oxidation Resistance of Gold-Coated Iron Nanoparticles. *Chemistry of Materials,* **17**: 3181-3186.

Dièguez, O., Alemany, M.M.G., Rey,C., Ordejon, P & Gallego, L.J. 2001. Density-functional calculations of the structures, binding energies, and magnetic moments of Fe clusters with 2 to 17 atoms. *Phys. Rev. B,* **63(20)**:205407.

Guevara, J., Llois, A.M & Weissmann, M. 1998. Large variations in the magnetization of co clusters induced by noble-metal coating. *Phys. Rev. Lett.,* **81**:5306-5309.

Ganteför, G & Eberhardt, W. 1996. Localization of *3d* and *4d* Electrons in Small Clusters: The "roots" of magnetism. *Phys. Rev. Lett.,* **76**:4975.

Hagos W. G & Anjali, K. 2007a. Adsorption of molecular hydrogen and hydrogen sulphide on Au clusters. *J. Chem. Phys.,* **126**:244705.

Hagos W. G & Anjali, K. 2007b. How cationic gold clusters respond to a single sulfur atom. *J. Chem. Phys.,* **127**:224708.

Häkkinen, H., Barnett, R. N & Landman,U. 1999. Electronic Structure of Passivated Nanocrystal. *Phys. Rev. Lett.,* **82**:3264-3267.

Häkkinen, H & Landman,U. 2000. Gold clusters and their anions. *Phys. Rev. B,* **62**:R2287-R2289.

Hohenberg, P & Kohn, W. 1964. Inhomogeneous Electron Gas. *Phys. Rev. B,* **136**:864.

http://www.pwscf.org, (PWSCF code in Quantum-Espresso).

Khmelevskyi, S., Kudrnovsky, J., Gyory, B.L., Mohn, P., Drchal, V & Weinberger, P. 2004. Frustration and long-range behavior of the exchange interactions in AuFe spin-glass alloys. *Phys. Rev. B,* **70:**224432.

Kohn, W & Sham, L. 1965. Self-Consistent Equations Including Exchange and Correlation Effects. *J. Phys. Rev.,* **140**:A1133**.**

Kinoshita, T., Seino, S., Mizukoshi,Y., Otomea,Y., Nakagawa, T., Okitsud, K & Yamamoto, T.A. 2005. Magnetic Separation of Amino Acids by Gold/Iron-Oxide Composite Nanoparticles Synthesized by Gamma-ray. *J. Magn. Magn. Matter,* **293**:106.

Kittel, C. 1996. Introduction to Solid State Physics. 7th Edition, Wiley, New York, 673p.

Lin, J., Zhou,W., Kumbhar,A., Wiemann, J., Fang, J., Carpenter, E.E & `Connor, C.J. O. 2001. Gold-Coated Iron (Fe@Au) Nanoparticles: Synthesis, Characterization, and Magnetic Field-Induced Self-Assembly. *J. Solid State Chem.,* **159**:26-31.

Majumdar, C & Kulshreshtha, S.K. 2006. Structural and electronic properties of Au_n (n=2–10) clusters and their interactions with single S atoms: *Ab initio* molecular dynamics simulations. *Phys. Rev. B,* **73**:155427.

Mornet, S., Vasseur, S., Grasset, F & Duguet, E. 2004. Magnetic nanoparticle design for medical diagnosis and therapy. *J. Mater. Chem.,* **14**:2161.

Ortega, D & Pankhurst, Q.A. 2013. Magnetic hyperthermia, in Nanoscience: Nanostructures through Chemistry. *Royal Society of Chemistry,* **1**: 63-64.

Palots, K., Lazarovits, B., Szunyogh, L & Weinberger, P. 2004. *Ab initio* study of the electric transport in gold nanocontacts containing single impurities. *Phys. Rev. B,* **70**:134421.

Purdum, H., Montano, H.A., Shenoy, G.K & Morrison, T. 1982. Extended x-ray absorption fine structure study of small Fe molecules isolated in solid neon. *Phys. Rev. B,* **25**:4412.

Pyykkö, P. 1988. Relativistic effects in structural chemistry. *Chem. Rev.*, **88(3)**:563-594.

Sun, Q., Kandalam,A.K., Wang, Q., Jena, P., Kawazoe, Y & Marquez, M. 2006. Effect of Au coating on the magnetic and structural properties of Fe nanoclusters for use in biomedical applications: A density-functional theory study. *Phys. Rev. B,* **73:**134409-134414.

Sun, Q., Reddy, B.V., Marquez,M., Jena, P., Gonzalez, C & Wang, Q. 2007. Theoretical Study on Gold-Coated Iron Oxide Nanostructure: Magnetism and Bioselectivity for Amino Acids. *J. Phys. Chem. C,* **111(11)**:4159-4163.

Sun, Q., Wang,Q., Rao, B. K & Jena, P. 2004. Electronic structure and bonding of Au on SiO_2 cluster: A nano bullet for tumors. *Phys. Rev. Lett.*, **93(18)**:186803.

Vijay K. Varadan, LinFeng Chen & Jining Xie. 2008. Nanomedicine: Design and Applications of Magnetic Nanomaterials, Nanosensors and Nanosystems. ISBN: 978-0-470-03351-7, Wiley and Sons, New York, 484 p.

Vosko, S.H., Wilk, L & Nusair, M. 1980. Accurate spin-dependent electron liquid correlation energies for local spin density calculations: a critical analysis. *Can. J. Phys.*, **58(8)**:1200-1211.

Wang, Q., Sun, Q., Yu, J.Z., Hashi,Y & Kawazoe, Y. 2000. First-principles studies on magnetism of Ni clusters coated and alloyed with Pd. *Phys. Lett. A,* **267**:394.

Wang, Y & Perdew, 1991. Correlation hole of the spin-polarized electron gas, with exact small-wave-vector and high-density scaling. *Phys. Rev. B,* **44**:13298-13307.

Zhang, N., Hayase, T., Kawamata, H., Nakao, K., Nakajima, A & Kaya, K. 1996. Photoelectron spectroscopy of iron-sulfur cluster anions. *J. Chem. Phys.,* **104**:3413-3419.